J.Natn.Sci.Foundation Sri Lanka 2023 51 (3): 541 - 555
DOI: http://dx.doi.org/10.4038/jnsfsr.v51i3.11380

RESEARCH ARTICLE

Atmospheric Science

Variations of pre-monsoon season related atmospheric parameters over Kakinada region

TR Vishnu[1], KS Kumar[2], SKH Ahammad[2], GNS Kumar[3], N Umakanth[4], MC Rao[5*] and S Krishna[6]

[1] *Department of Electronics and Communication Engineering, Priyadarshini Institute of Technology and Science For Women, Chintalapudi, India.*
[2] *Department of Electronics and Communication Engineering, Koneru Lakshmaiah Education Foundation, Vaddeswaram, India.*
[3] *Department of Mechanical Engineering, R K College of Engineering, Amaravathi, India.*
[4] *Department of Electronics and Communication Engineering, Kallam Haranadhareddy Institute of Technology, Chowdavaram, India.*
[5] *Department of Physics, Andhra Loyola College, Vijayawada, India.*
[6] *Department of Electronics and Communication Engineering, Dhanekula Institute of Engineering and Technology, Vijayawada, India.*

Submitted: 03 August 2022; Revised: 27 March 2023; Accepted: 28 April 2023

Abstract: Pre-monsoon showers occur before the beginning of the rainy season. From the months of March to May, they take place, and can be anything from little drizzles to powerful thunderstorms. March, April and May are known as the pre-monsoon season (PRMS). The precipitation patterns recorded in PRMS are critical because they have an impact on a wide range of crop-related operations across the country. During PRMS, the maximum temperature (TMAX), minimum temperature (TMIN), soil moisture, relative humidity, latent heat, convective available potential energy (CAPE), and total precipitable water (TPW) were analysed at Kakinada region. These variables were collected using daily ERA5 reanalysis data for the PRMS from 1981 to 2021. Studying the convection-related characteristics over the Kakinada station during the PRMS was our goal. During the study period, the five years with the highest PRMS rainfall were 1990, 1995, 2008, 2010 and 2016 and the five years with the lowest rainfall were 1990, 1995, 2008, 2010 and 2016. In the months leading up to the monsoon, the Kakinada station experiences CAPE values between 1000 and 6000 J/kg, while TPW values are between 25 and 60 mm. The PRMS values for CAPE and TPW both show that the prerequisites for moderate to severe convection activity have been fulfilled. TPW, soil moisture, relative humidity, and CAPE parameters during PRMS were well estimated using the ARMA and ARIMA models.

Keywords: Convection, pre-monsoon, soil moisture, total precipitable water.

INTRODUCTION

PRMS (March-May) in India is a transitional period between the winter and monsoon seasons (Ray *et al*., 2016). The monsoon season usually begins in advance of the month of June and continues till the end of September across the Indian region (Tyagi *et al*., 2019). Thunderstorms have become increasingly regular in recent years and they have been accompanied by heavy rain and lightning strikes. Every year, these thunderstorms kill hundreds of people and destroy vast quantities of property. Hundreds of people are being affected by thunderstorm activity in India every year. In 2022, till November, 907 people were dead due to thunderstorm events that occurred over different regions (The Hindu, 2023). A high death rate is observed in West Bengal, Jharkhand, Bihar, Assam, and Odisha states. The common scenario which we observe during these events is a large growing cloud. These systems occur from a small area to larger areas depending on the local instability that triggers the thunderstorm events (single cell or multi-cell) (Bharadwaj *et al*., 2017).

The instability is caused by the heating of the land surface. This heating makes the air warm and moist. This air collides with the oceanic air mass. Numerous studies have been conducted on the PRMS thunderstorms and other convective events in northern India. In moisture advection phenomena, the southerly winds are absent. This was investigated by Srinivasan (1962) and he found that the Gangetic West Bengal region experiences more

* Corresponding author (raomc72@gmail.com; https://orcid.org/0000-0001-9136-9679)

favourable convection conditions for thunderstorm occurrences. In a few occasions, though the favourable situations exists, convection initiation does not takes place in the region of occurrence. Srinivasan *et al*. (1973) discovered that heavy rainfall periods in northern India are linked to horizontal scale westerly trough winds that supply a good moisture content to the PRMS convective zone, despite the fact that the westerly continental airflow contributes limited precipitation.

The convection linked systems over eastern India and Bangladesh are of the squall line type of convection, which causes high winds and precipitation (Rafiuddin *et al*. 2009). The squall line is one of the forms of convective storms that lead to hail storm and tornado activity in eastern parts of India (Bhattacharya & Bhattacharya, 1983). They also determined that storm seasons are usually associated with convection variations that occur due to heating activity that take place in the lower atmospheric pressure levels. There is a lot of lightning during these severe convective storms. Nor'westers that possess high surface wind speeds which are greater than 50 km h^{-1} have high counts of lightning strikes, *i.e.*, 30 per minute on a regular basis (Midya *et al*., 2021). They also discovered that the lightning strikes keep increasing rapidly before 10–40 minutes of onset of the convective storm. According to Chaudhuri (2008), cumulonimbus and stratocumulus clouds are the most commonly seen clouds over eastern parts of India during the PRMS. According to Nayak and Mandal (2014), energy-helicity index, wind shear parameter derived between 3 and 7 km s^{-1}, and the vorticity generation parameters play a critical role in the assessment of thunderstorm precipitation. Roy (2021) discovered three areas in the Indian subcontinent having maximum thunderstorm occurrences. They identified those areas by analysing long-term patterns in thunderstorm frequency. They also revealed that in the second part of the twentieth century, the frequency of thunderstorm days in eastern and southern India is dropping. But in the recent two decades they were increasing at an abnormal rate, which is due to the effect of global warming. Thunderstorms were most common at night in north-eastern India, whereas they were most common in the evening in eastern India, according to Ray *et al*., 2016. They also determined that thunderstorms occur often at night in the sub-Himalayan West Bengal and Sikkim regions. However, the Odisha, Bihar, and West Bengal states have suffered more thunderstorm occurrences in the evening times (Ravi *et al*., 1999; Tyagi *et al*., 2011). Several studies were conducted to see how well various stability criteria predicted favourable circumstances for convection to form and develop into thunderstorms (Schultz, 1989; Kunz, 2007; Dhawan *et al*., 2008).

CAPE is a great predictor of convection activity over eastern India, and it's also great for operational forecasting (Roy *et al*., 2008). This indicator gives information on buoyant energy in the atmosphere as well as wet instability (Neelin, 1997). Numerous studies were published on convection based events during monsoon time.

Kakinada is the state's sixth largest city and the district headquarters of the East Godavari district in Andhra Pradesh, India. On the Bay of Bengal's coast, it is located at 16.93ºN latitude and 82.22ºE longitude. Kakinada has a tropical, dry climate with hot, humid weather for the majority of the year. With maximum temperatures of 38–42 °C, late May and early June are the warmest months of the year. The coldest month is January with minimum temperatures of 18–20 °C. The southwest monsoon provides the majority of the city's seasonal rainfall; however the northeast monsoon also provides significant rain (from mid-October to mid-December). The city is frequently hit by cyclones from the Bay of Bengal. The prevalent winds in Kakinada are southwest throughout the most of the year, except from October to January, when they are northeast. The average annual rainfall in the city is 110–115 mm (Seatemperature.org). There is very little comprehensive research on PRMS related convective systems, that employs long-term information from across the study region. This study looks at convection-related characteristics over the Kakinada station in the Andhra Pradesh region during PRMS. These pre-monsoon convective systems are responsible for a large number of deaths and property damage in this region and so require additional research. The purpose of this research is to close that gap. Forecasting mesoscale convective activity, particularly pre-monsoon convective episodes and related rainfall, is also a key difficulty for the forecasting community. The goal of this research is to find out what factors influence convective systems above the Kakinada station during the PRMS.

MATERIALS AND METHODS

Data

The GPM IMERG (Integrated Multi-satellite Retrievals for Global Precipitation Measurement) system is a well-defined US mechanism for sending multi-satellite precipitation data to the GPM team in the United States. The Goddard Profiling Algorithm is used to grid, intercalibrate, and integrate the GPM constellation's many precipitation-relevant satellite passive microwave (PMW) sensors into half-hourly 0.1° x 0.1° (about 10 x 10 km) fields (GPROF2017). These data are accessible from any location on the globe. The URL *https://gpm.nasa.gov/data/directory/index.html* contains the GPM IMERG data. For the years 1981 to 2021, 0.25° precision ERA5 surface level and pressure level reanalysis data were obtained (Hersbach & Dee, 2018); *https://cds.climate.copernicus.eu/#!/home* is the URL where ERA5 data are collected. The National Oceanic and Atmospheric Administration's (NOAA) Global Reanalysis Products provided us with information on soil moisture, relative humidity, maximum temperature, minimum temperature, and latent heat flux. These data are available at *https://psl.noaa.gov/data/gridded/data.ncep.reanalysis.html.* The NASA Global Modeling and Assimilation Office has released MERRA-2, or Modern-Era Retrospective Analysis for Research and Applications (Gelaro *et al*., 2017). The original MERRA atmospheric reanalysis dataset has been replaced and expanded with this updated, higher-quality output of the global reanalysis (Rienecker *et al*., 2011). The Modern-Era Retrospective Analysis for Research and Applications version 2 (MERRA-2) was used to gather daily temperature data over Kakinada region from 1981 to 2021. MERRA2 data can be found at *https://goldsmr4.gesdisc.eosdis.nasa.gov/data/MERRA2*.

Methodology

We have used the calculations below to determine the CAPE and TPW parameters using the above data.

CAPE

CAPE is a unit of measurement for the potential energy of an air parcel per kilogramme of air mass, which is expressed in Joules per kilogramme (J/kg). CAPE refers to the buoyant energy necessary to lift an air packet into the air. When you combine these two numbers together, you get the total positive buoyant energy from free convection to equilibrium (Moncrieff & Miller, 1976).

$$\text{cape} = \int_x^y g[\frac{TV_{parcel} - TV_{env}}{TV_{env}}]\, dz \quad \ldots(1)$$

Where TV_{parcel} and TV_{env} denote the parcel's virtual temperature and the environment's virtual temperature, respectively, x and y reflect the levels of free convection and neutral buoyancy.

Cape parameter critical values (Grieser, 2012)

Cape (in J/kg)	Thunderstorm chances
Under 300	No energy for convection
From 300 to 1000	Weak convection has a low potential.
From1000 to 2500	Convectional potential is moderate.
Greater than 2500	Convectional potential is high.

Total precipitable water (TPW)

The quantity of water that can be collected from the earth's surface to the topmost pressure level in the atmosphere is determined using TPW. When all of the water and water vapour has condensed into a liquid phase, this should satisfy the following formula, which is used to calculate it.

$$TPW = \frac{1}{g}\int_{P_1}^{P_2} W\ dP \quad \ldots(2)$$

W is the mixing ratio and P_1 and P_2 are the two pressure levels (Carlson *et al*., 1990).
The basic arithmetic equation for the ARMA model is as follows:

$$X(t) = \sum_{i=1}^{p} \theta_i X(t-i) + \sum_{j=1}^{q} \emptyset_j e(t-i) \quad \ldots(3)$$

Where $\theta_i, \emptyset_j$ are the autoregressive and moving average coefficients, respectively.
p, q: Autoregressive and Moving Average order.
X_t : Values of output parameters at time t for t = 1, 2, 3, ... t,
e_t: White noise

The numerical representation of the Autoregressive operator is as follows:

$$\theta_i = \theta_1 X(t-1) + \theta_2 X(t-2) + \cdots + \theta_p X(t-p) \quad \ldots(4)$$

In the same way, the moving average operator is defined as

$$\emptyset_j = \emptyset_e(t-1) + \emptyset_e(t-2) + \cdots + \emptyset_p e(t-q) \quad \ldots(5)$$

The autoregressive and moving average coefficients are computed using the Yule-Walker and Newton-Raphson relations (Ratnam *et al*., 2019). The ARMA estimation model that we utilized in this work was trained and tested using the MATLAB 7.0 Toolbox.

The ARIMA (auto regressive integrated moving average) model was created as an extension or generalisation of the ARMA model (Box and Jenkins 1976). ARIMA (p, d, q) is made up of three parts: autoregressive (AR), integrated (I), and moving average (MA) (MA). The letter p stands for the AR component. It illustrates the consequences of previously stretched PRMS data. The letter d stands for the integrated (I) component. It demonstrates the wide range of differences. Finally, q is used to represent the MA component. The ARIMA (p, d, q) model is given as follows in its most basic form (Box & Jenkins, 1976; Brockwell & Davis, 2001).

$$\emptyset_p(B)(1-B)^d V_t = \theta_q(B)\varepsilon_t \quad \ldots(6)$$

Where $\theta_p, \emptyset_q$ are the autoregressive and moving average coefficients, respectively.
p, q : Autoregressive and moving average order.
V_t : Forecasted output parameter values at time t
d : The number of times the data has been changed
B : Operator for the backward shift $BV_t = V_{t-1}$
ε_t : Error term, a normal distribution with mean 0 and standard deviation 2

It is crucial that a model be used to examine the performance of ERA5 data in order to test the significance of PRMS parameters and to create confidence intervals for the estimation. Finally, an estimation is made using the ARMA and ARIMA models. For the ARMA and ARIMA estimation methods, the PRMS parameters were used. Finding the stochastic process of the time series and properly predicting future values are the major goals of fitting the ARIMA model. First, adequate values for p, q, and d, three parameters of the ARIMA model, were identified. The statistical toolbox in MATLAB 2018 is the software utilized for ARMA and ARIMA models. Time series forecasting is a rapidly expanding field of study, offering numerous opportunities for new research in the future. One of them is the 'Combining Approach,' in which a variety of various and unrelated methodologies are combined to increase forecast accuracy.

We generated BIAS, correlation coefficient (CC), and root-mean-square error (RMSE) terms for various parameters to statistically analyse the ARMA and ARIMA model performances with ERA5 reanalysis data. Wilks (2006) gave the following formulas:

$$\text{BIAS} = \frac{1}{n}\sum_{i=1}^{n}(o_i - f_i) \quad \ldots(7)$$

$$\text{CC} = \frac{\sum_{i=1}^{n}(f_i - \acute{f})(o_i - \acute{o})}{\sqrt{\sum_{i=1}^{n}(f_i - \acute{f})^2}\sqrt{\sum_{i=1}^{n}(o_i - \acute{o})^2}} \quad \ldots(8)$$

$$\text{RMSE} = \sqrt{\frac{\sum_{i=1}^{n}(f_i - o_i)^2}{n}} \quad \ldots(9)$$

Where o_i and f_i are the observed and predicted values, respectively.

RESULTS AND DISCUSSION

The characteristics impacting PRMS convective systems at the Kakinada station were investigated in this study. During the period 1981–2021, we have calculated the PRMS mean rainfall for each year at the Kakinada station (Figure 1). 1990, 1995, 2016, 2010, and 2008 are the years with the five highest PRMS rainfall over the study region. 1991, 1985, 2017, 1982, and 1996 are the five lowest PRMS rainfall years over the study region. The mean PRMS daily rainfall from the GPM-IMERG satellite output is shown in Figure 1. Based on available daily rainfall data from the Kakinada station for the years 1981 to 2021, the mean seasonal rainfall across the PRMS is around 110 mm. During the PRMS month of May, the most intense convection activity is observed (see Figure 1). The years 1990, 1995 and 2016 showed rainfall higher than the normal mean rainfall. In these three years, there was cyclonic activity which led to high rainfall occurrence on the Kakinada region.

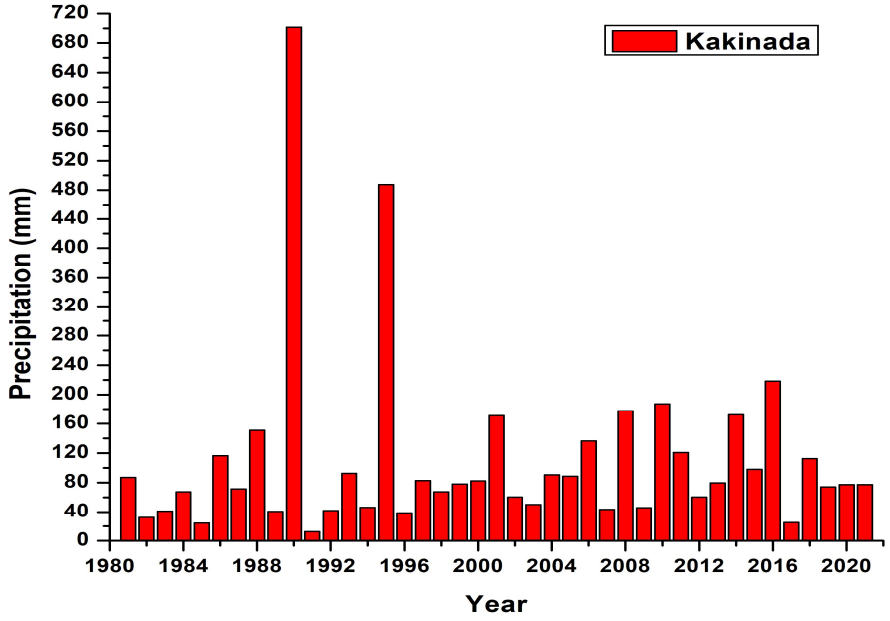

Figure 1: Mean PRMS rainfall variations over the Kakinada station during the time period 1981 -2021.

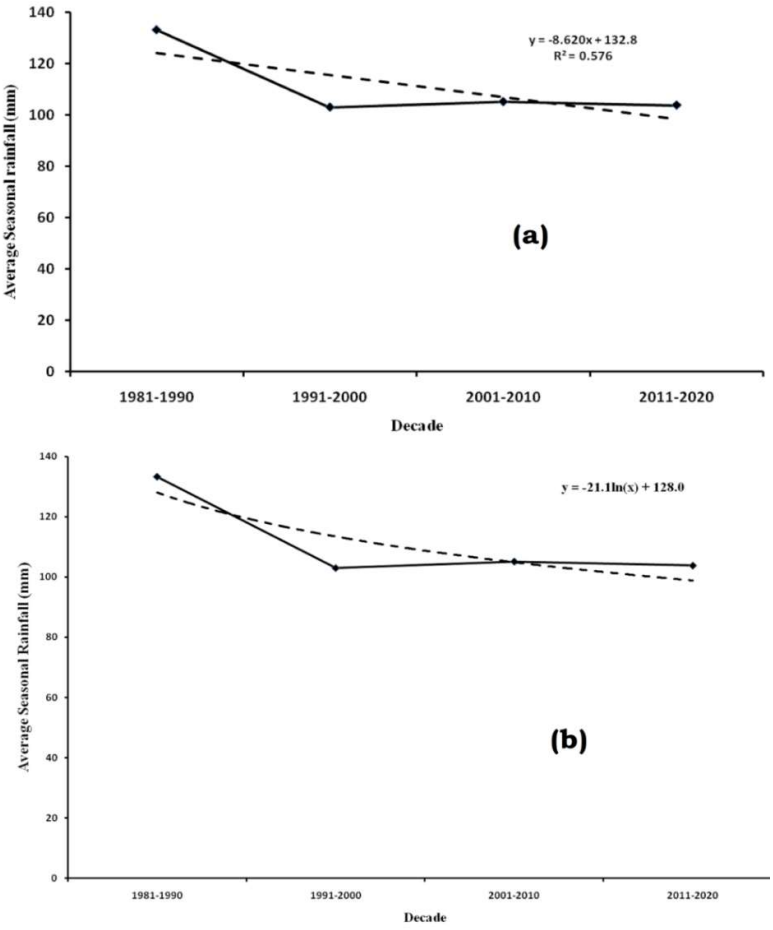

Figure 2: Decadal variation of average seasonal rainfall over the Kakinada station.

From 1991 to 1994 and 1996 to 2000, the average seasonal rainfall has decreased each year. (See Figure 1 for further information). Rainfall activity has also increased from 2005 to 2021. A deceasing trend has been noticed in the decadal variation of average seasonal rainfall during 1981-2021 (see Figure 2a and b).

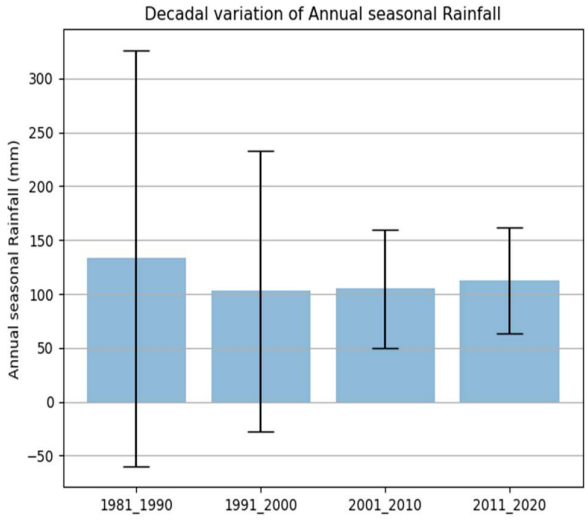

Figure 3: Bar plot of average seasonal rainfall with error bars over the Kakinada station.

Error bars are useful to problem solvers because they reflect the confidence or precision in a collection of measurements or calculated results. The generated plot has four error bars. Looking at the error by duration, we can observe that the standard deviation of seasonal rainfall during 1981-1990 is larger than the standard deviation of seasonal rainfall throughout other decades (Figure 3).

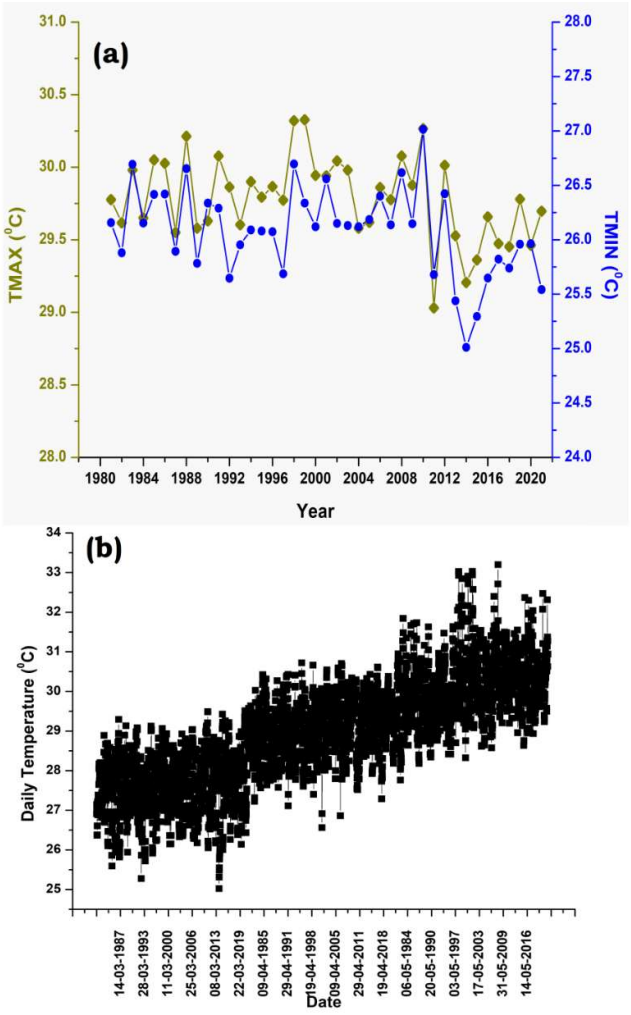

Figure 4: (a) Variations of maximum temperature parameter and minimum temperature parameter during the period 1981- 2021 of the PRMS at Kakinada region; (b) Daily Variations of temperature parameter during the period 1981- 2021 of the PRMS at Kakinada region.

The time series of maximum and minimum temperatures for the PRMS are presented in Figure 4a. The TMAX values over Kakinada station during all PRMS months range from 29 to 32 ºC. It was seen that when the TMAX values are decreasing, the rainfall is increasing. The rainfall occurrence in May has been severe in the last five years, indicating strong rainfall activity over the Kakinada region. TMIN values over Kakinada station range from 25 to 27 ºC for all the PRMS months. In the recent 5 years there is a drop in TMIN values which is favouring high rainfall occurrence during PRMS over the Kakinada region. Rainfall activity in the Kakinada region is higher in the months of April and May than it is in the month of March. The daily temperature values are higher in May when compared to March and April. In March, the average temperature values range between 25 ºC and 29 ºC. In April, the average temperature values range between 26 ºC and 31 ºC and between 27 ºC and 33 ºC in May (Figure 4b). When sunlight and infrared radiation heat the Earth's surface, water condenses as buoyant air rises, forming convective systems. As CO_2 levels rise and the land surface heats, stronger updrafts are more likely to produce lightning and rainfall.

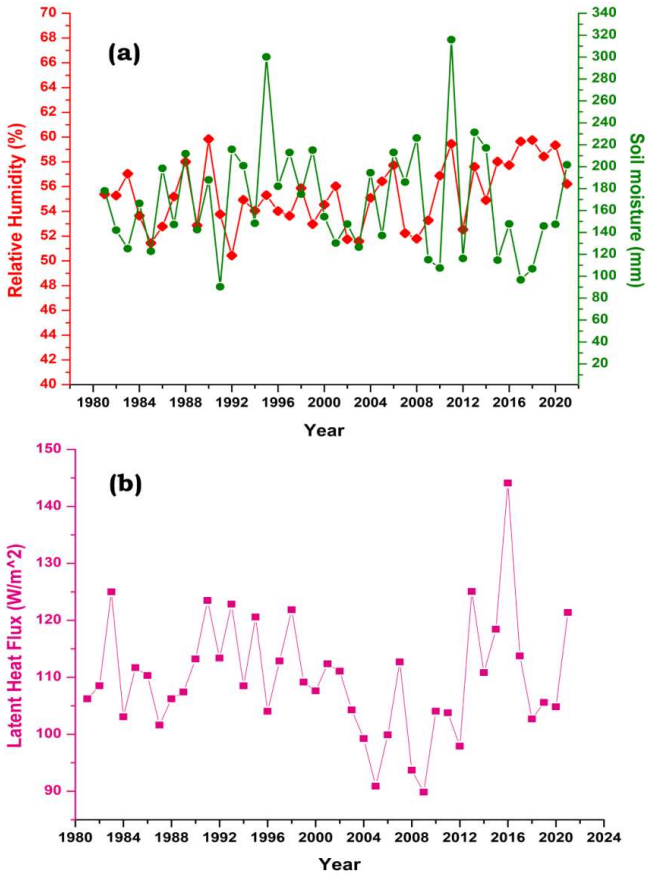

Figure 5: Variations of (a) soil moisture and relative humidity parameter; (b) latent heat flux parameter during the period 1981- 2021 of the PRMS at Kakinada region.

Temperature and precipitation forecasts rely heavily on soil moisture. The rate of evaporation of soil moisture increases as the temperature rises. The increased evaporation of soil moisture aids in ground cooling. Convective precipitation is influenced by soil moisture in two ways. Evaporation is aided by increased soil moisture, which cools the surface while also supplying moisture to the atmosphere. Cooling would limit convection and consequently precipitation, but adding moisture would increase precipitation. The time series of soil moisture for PRMS is displayed in Figure 5a. Over Kakinada station, soil moisture readings range from 80 to 330 mm for all the PRMS months. When the soil moisture value rises, then the rainfall rises with it. In the recent 5 years, the soil moisture values have increased significantly. This helps the high rainfall activity over the Kakinada region. Thunderstorms and convective systems thrive in high-humidity conditions. Convective systems are strengthened substantially when rising humid air cools in the higher regions of the storm, because they are tall weather systems based on columns of rising air. All of the heat energy used to evaporate that water is released as the cooling humidity condenses into liquid water in the clouds. This extra heat warms the air around it, making it more buoyant. This relative humidity parameter helps to increase the peak stage of convective formation. The time series of relative humidity for the PRMS is displayed in Figure 5a. Over the Kakinada station, the mean relative humidity values range from 50 to 60% during all the PRMS months. These percentages reached 90% on convection days. In thunderstorms and hurricanes, latent heat is extremely essential. Warm air rises, and the water vapour contained therein condenses onto cloud condensation nuclei, generating clouds. At this point, the air has become saturated. When the water vapour in this air first begins to rise, it is in the gaseous phase. Latent heat is released into the atmosphere as water vapour condenses into clouds. The latent heat then causes instability by warming the surrounding air around the nascent cloud droplet. Warm air in the vicinity of the cloud droplet will now desire to climb and condense. The time series of latent heat flow for the PRMS is displayed in Figure 5b. The latent heat flux measurements over the Kakinada station range from 85 to 150 W/m^2 during the PRMS months.

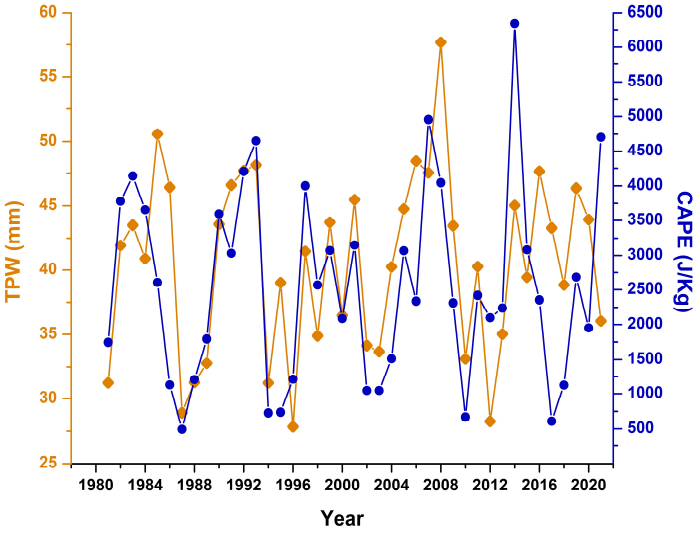

Figure 6: Variations of CAPE parameter & TPW parameter during the period 1981- 2021 of the PRMS at Kakinada region.

We have computed CAPE and TPW values over the Kakinada region using ERA5 temperature and relative humidity data at various pressure levels. Time series plots of CAPE and TPW parameters for the PRMS from 1981 to 2021 are shown in Figure 6. In recent decades, the convective available potential energy (CAPE) has gained popularity as a prominent instability indicator for analysing the atmosphere's convective potential. It has been used in a number of studies and is calculated using an integral of a vertical cloud buoyancy profile. Total precipitable water is the amount of moisture that falls over a certain place (TPW). It represents the amount of moisture in the air rather than the amount of rain that will fall. During the pre-monsoon months, CAPE values over the Kakinada station vary from 1000 to 6000 J/kg, whereas TPW values range from 25 to 60 mm. Both the CAPE and TPW parameters in the PRMS demonstrate that the thresholds for moderate to severe convection activity are good.

Around 1000 and 950 hPa, there is a small dew point dip. At 800 hPa, it climbed to 6-14 K, then began to grow to 20 K at 500 hPa. It decreased to 12K at 250 hPa in March. In April and May, the values soared even at 200 hPa. This clearly shows that moist air occurs between 1000 hPa and 800 hPa, with dry air existing above it from (800 -500 hPa), and that moist air exists between 500 hPa and 400 hPa, with dry air existing in the upper layers of the atmosphere, reflecting a highly unstable situation over Kakinada station (Figure 7a). A plot of vertical velocity (VV) across the Kakinada area is given in Figure 7b. We saw big negative vertical velocity readings on days with a lot of convection. This suggests that air mass is moving higher in the lower atmosphere. When compared to April, the month of May saw more negative VV values. When negative VV values are seen, it means the air mass is ascending. When positive VV values are detected, it indicates that the air mass is sinking. This is owing to the fact that as height increases, pressure is lowered. The substantial moisture buildup across the study region supports these VV values on heavy precipitation days.

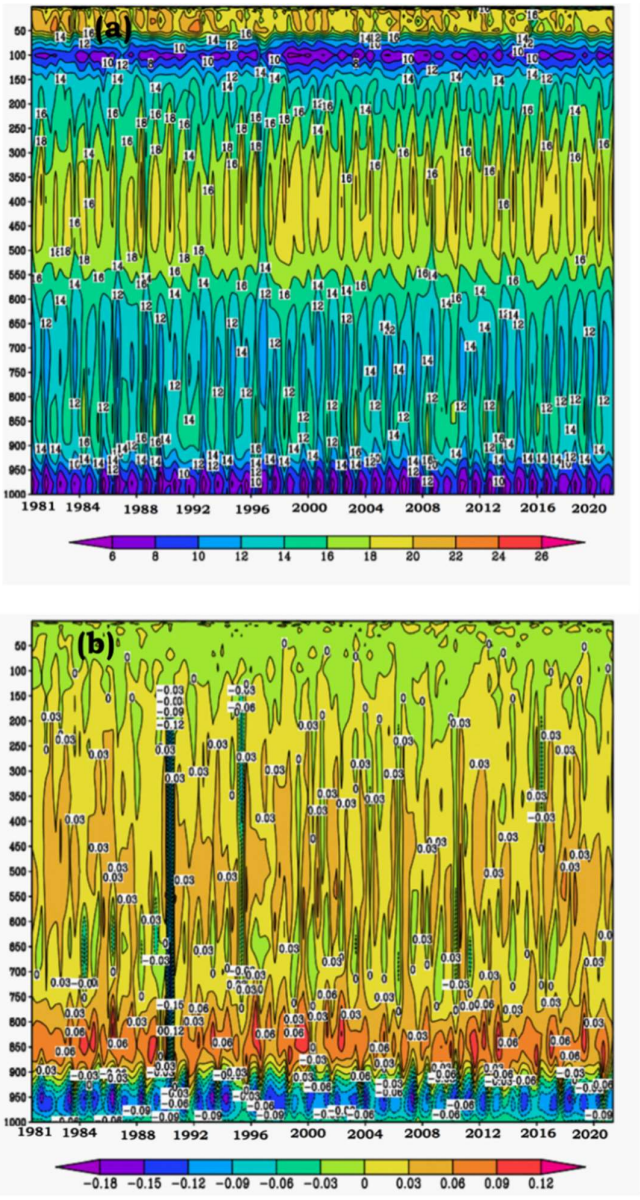

Figure 7: Time-height sections of (a) Dew point depression; (b) Vertical velocity during the period 1981- 2021 of the PRMS at Kakinada region.

In the Kakinada region, mean temperature and humidity profiles, computed from ERA5 measurements at various isobaric levels, were displayed (Figure 8a). As a result, these profiles can reveal how convection develops. The dew point depression is around 3K at 1000 hPa, then drops to 1K at 950 hPa, then rises to 8K at 700 hPa, then drops to 5K at 500 hPa, then rises to 14.5 K at 250 hPa, then drops to 5K at 100 hPa. This clearly implies that moist air exists between 1000 and 800 hPa, and that dry air exists above this moist air from 800 to 500 hPa, and that moist air exists between 500 and 400 hPa, and that dry air exists in the top layers of the atmosphere, indicating a very unstable environment (Figure 8b).

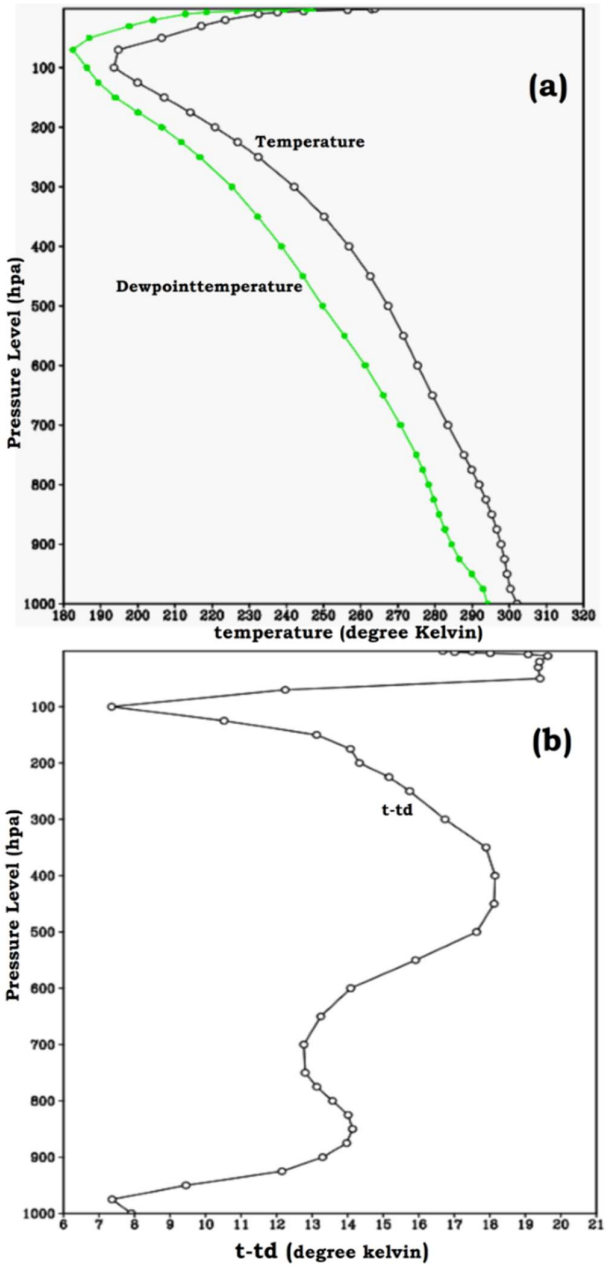

Figure 8: Time-height sections of (a) Temperature and dewpoint temperature parameters; (b) dewpoint depression during the period 1981- 2021 of the PRMS in the Kakinada region.

In the Kakinada region, the mean wind speed values from ERA5 measurements at various isobaric levels were displayed for PRMS (Figure 9a). At a height of ten metres above the Earth's surface, this value represents the greatest wind gust at the specified time. This metric is calculated by averaging the greatest wind speed over three seconds. As a result, these profiles reveal that the wind speeds increase slowly from surface to 500hpa. At the surface the wind speeds in PRMS are 4 to 6 m/s. From 500 hPa to 150 hPa, the wind speeds started increasing faster till 100 hPa. The wind speed values range in between 6 m/s and 19 m/s. This demonstrates that warm moist air is available in the lower levels whereas cold dry air is available in the upper levels. Cold dry air is related to westerly wind which we observe usually in PRMS. The warm moist air is usually linked to the Bay of Bengal. We also plotted PRMS surface wind speeds. These values range between 2.5 m/s and 4.3 m/s (Figure 9b).

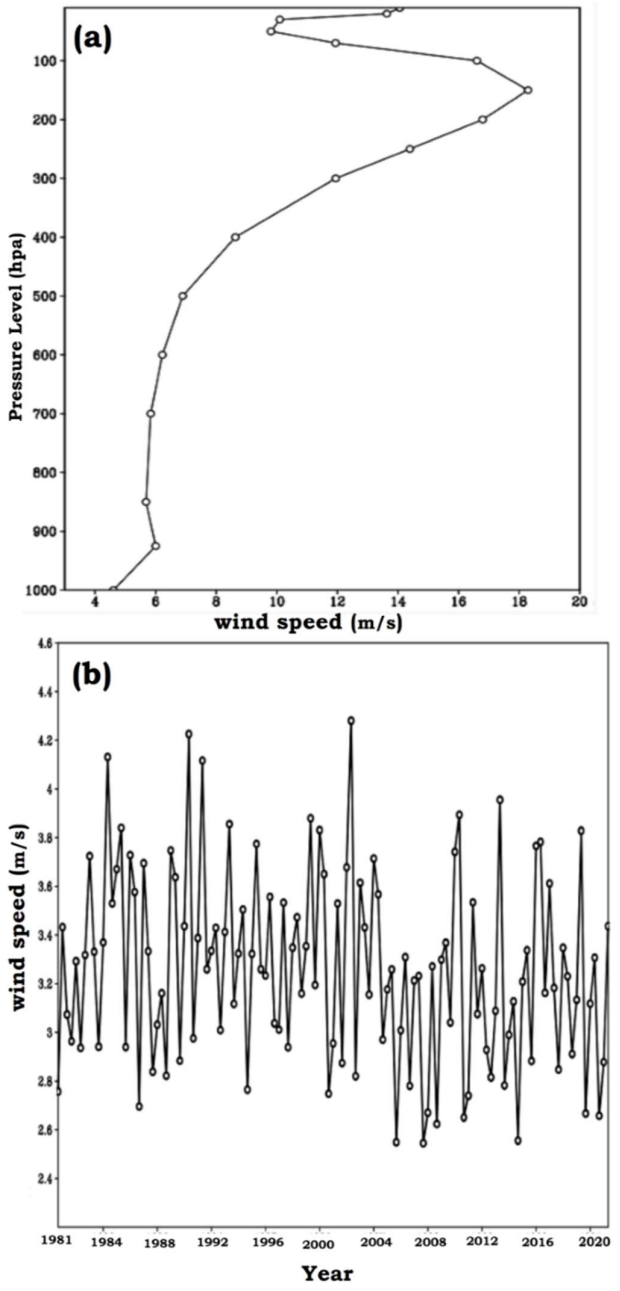

Figure 9: (a) Time-height sections of wind speed parameter; (b) Time series plot of 10 m-wind speed parameter during the period 1981- 2021 of the PRMS at Kakinada region.

We have chosen four factors (CAPE, TPW, relative humidity, and soil moisture) for ARMA and ARIMA model estimations based on their threshold values. As a result, we calculated those four parameters using the ARMA and ARIMA models. The main goal of this computation, as shown in Figure 10, is to compare the precision of ARMA and ARIMA models with ERA5 data.

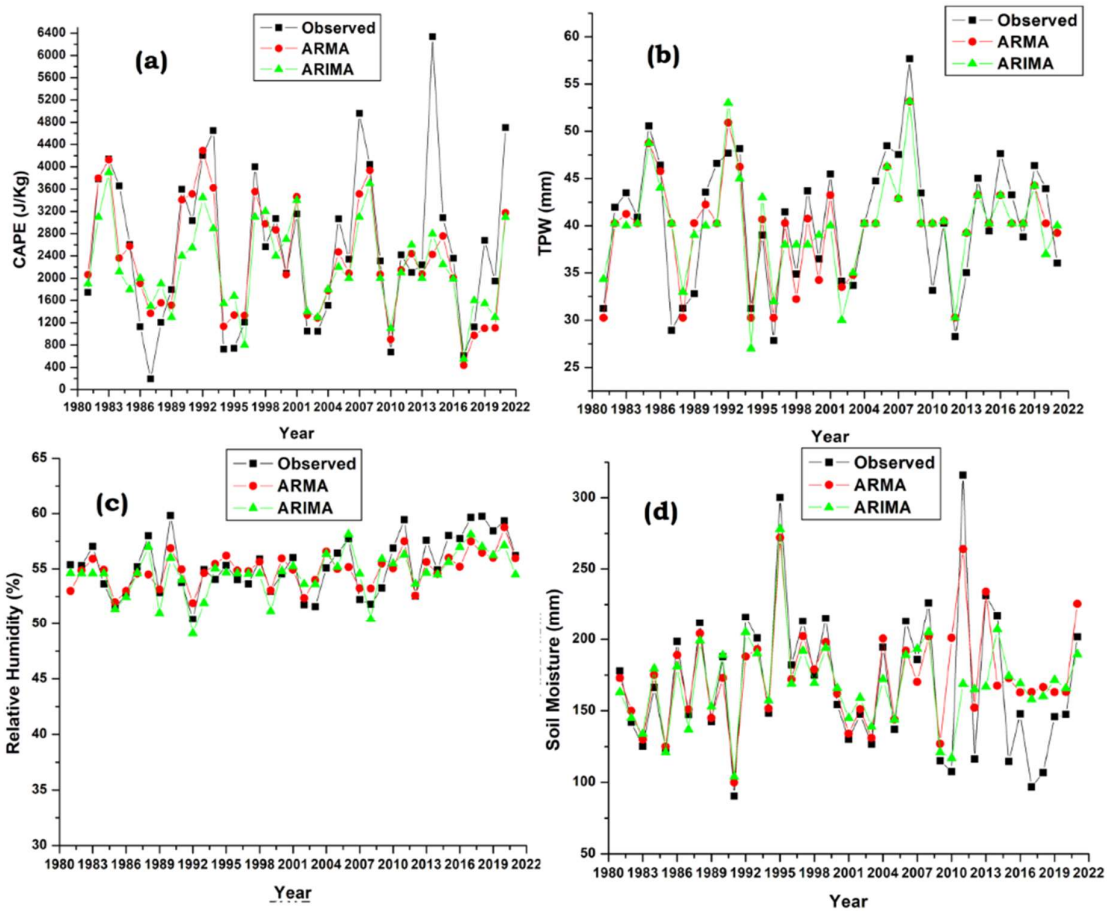

Figure 10: Time series plot of observed and calculated data for PRMS parameters (a) CAPE; (b) TPW; (c) Relative Humidity and (d) Soil Moisture, at Kakinada station from 1981 to 2021.

Table 1: Statistical Based analysis of ERA5 data and ARMA model

Parameter	RMSE	CC	BIAS
TPW	3.50	0.86	0.47
CAPE	863.0	0.80	220
Relative Humidity	1.64	0.81	0.39
Soil moisture	28.09	0.84	4.34

Table 2: Statistical Based analysis of ERA5 data and ARIMA model

Parameter	RMSE	CC	BIAS
TPW	4.15	0.79	0.51
CAPE	977.5	0.77	336.8
Relative Humidity	1.73	0.78	0.70
Soil moisture	33.39	0.76	0.85

A correlation analysis was done for the Kakinada station between the ERA5 computed values and the ARMA model computed values (Table 1). The ERA5 measured parameter values (observed) were compared to the ARIMA model calculated parameter values (Table 2). We calculated the BIAS, CC and RMSE for ARMA and ARIMA models, as shown in Tables 1 and 2. The TPW parameter has the highest CC of 0.86 when compared to

other components, meaning that 86 percent of the ARMA projected TPW complement the observed data (ERA5). The CC of the CAPE parameter is 0.77, meaning that 77% of the ARMA-calculated CAPE complement the observed data (ERA5). As a result, the ARMA and ARIMA models have shown to be quite useful in obtaining precise statistical estimates of thunderstorm-related properties. In terms of estimating PRMS parameters, the ARMA model beat the ARIMA model.

CONCLUSION

The convection-related properties are studied over the Kakinada station during the PRMS. The current study is being carried out for the PRMS from 1981 to 2021. Both the CAPE and TPW metrics in the PRMS indicate that the conditions for moderate to severe convection activity are met. ARMA and ARIMA models can be used to produce a significant decision-making tool. The benefit of adopting this kind of models is that, despite many issues with their development and testing, we learn about the structure of the time series and the process that led to its production. It is fascinating to develop models for thunderstorm-related rainfall because of its intricate structure and sensitivity to environmental factors. The study demonstrates that the ARMA and ARIMA models are not only reliable but also the best models for predicting the activity of thunderstorms that produce rainfall. Policymakers are alerted by predicted outcomes to make the appropriate preparations in advance to deal with thunderstorm heavy rainfall events. As a result, the ARMA and ARIMA models have shown to be quite beneficial in obtaining precise statistical estimates of thunderstorm-related characteristics. When it comes to estimating PRMS parameters, the ARMA model outperformed the ARIMA model.

REFERENCES

Bhattacharya A.B. & Bhattacharya R. (1983). Radar observations of tornadoes and the field intensity of atmospherics. *Meteorology and Atmospheric Physics* **32**(1–2): 173–179.
DOI: https://doi.org/10.1007/BF02272722

Bharadwaj P., Singh O. & Kumar D. (2017). Spatial and temporal variations in thunderstorm casualties over India. *Singapore Journal of Tropical Geography* **38**(3): 293–312.
DOI: https://doi.org/10.1111/sjtg.12201

Box G.E. & Jenkins G.M. (1976). *Time Series Analysis: Forecasting and Control*, 2nd edition. Holden-Day Inc., San Francisco, USA.

Brockwell P.J. & Davis R.A. (2001). *Introduction to Time Series and Forecasting,* 2nd edition. Springer, New York, USA.

Carlson T.N., Perry E.M. & Schmugge T.J. (1990). Remote estimation of soil moisture availability and fractional vegetation cover for agricultural fields. *Agricultural and Forest Meteorology* **1-52**(1-2): 45–69.
DOI: https://doi.org/10.1016/0168-1923(90)90100-K

Chaudhuri S. (2008). Preferred type of cloud in the genesis of severe thunderstorms – a soft computing approach. *Atmospheric Research* **88**(2): 149–156.
DOI: https://doi.org/10.1016/j.atmosres.2007.10.008

Dhawan V.B., Tyagi A. & Bansal M.C. (2008). Forecasting of thunderstorms in pre-monsoon season over Northwest India. *Mausam* **59**(4): 107–111.
DOI: https://doi.org/10.54302/mausam.v59i4.1272

Gelaro R, McCarty W, Suárez M.J., Todling R, Molod A, Takacs L. & Zhao B (2017) The modern-era retrospective analysis for research and applications, version 2 (MERRA-2). *Journal of Climate* **30**(14): 5419–5454.
DOI: https://doi.org/10.1175/JCLI-D-16-0758.1

Grieser J. (2012). *Convection Parameters*. Selbstverl, Germany.

Hersbach H. *et al.* (15 authors) (2018). *ERA5 hourly data on single levels from 1979 to present.* Copernicus Climate Change Service (C3S) Climate Data Store (CDS). Available at *https://cds.climate.copernicus.eu/cdsapp#!/search?type=dataset.*

Kunz M. (2007). The skill of convective parameters and indices to predict isolated and severe thunderstorms. *Natural Hazards and Earth System Sciences* **7**: 327–342.
DOI: https://doi.org/10.5194/nhess-7-327-2007

Midya S.K., Pal S., Dutta R., Gole P.K., Chattopadhyay G., Karmakar S., Saha U. & Hazra S. (2020). A preliminary study on pre-monsoon summer thunderstorms using ground-based total lightning data over Gangetic West Bengal. *Indian Journal of Physics* **95**: 1–9.
DOI: https://doi.org/10.1007/s12648-020-01681-y

Moncrieff M.W. & Miller M.J. (1976). The dynamics and simulation of tropical cumulonimbus and squall lines. *Quarterly Journal of the Royal Meteorological Society* **102**(432): 373–394.
DOI: https://doi.org/10.1002/qj.49710243208

Nayak H.P. & Mandal M. (2014). Analysis of stability parameters in relation to precipitation associated with pre-monsoon thunderstorms over Kolkata India. *Journal of Earth System Science* **123**(4): 689–703. DOI: https://doi.org/10.1007/s12040-014-0426-z

Neelin J.D. (1997). Implications of convective quasi-equilibria for the large-scale flow. In: *Physics and parameterization of moist atmospheric convection* (ed. R.K. Smith) pp. 413–446. Kluwer Academic Publishers, London, UK. DOI: https://doi.org/10.1007/978-94-015-8828-7_17

Rafiuddin M., Uyeda H. & Islam Md. N. (2009). Simulation of characteristics of precipitation systems developed in Bangladesh during pre-monsoon and monsoon. *Proceedings of the 2nd International Conference on Water and Flood Management* (ICWFM-2009*)*, 15-17 March. Dhaka, Bangladesh, pp. 61–67. DOI: https://doi.org/10.1002/joc.1949

Ravi N., Mohanty U.C., Madan O.P. & Paliwal R.K. (1999). Forecasting of thunderstorms in the pre-monsoon season at Delhi. *Meteorological Applications* **6**: 29–38. DOI: https://doi.org/10.1002/met.19996103

Ratnam D.V., Otsuka Y., Sivavaraprasad G. & Dabbakuti J.K. (2019). Development of multivariate ionosphere TEC forecasting algorithm using linear time series model and ARMA over low-latitude GNSS station. Advances in Space Research **63**(9): 2848–2856. DOI: https://doi.org/10.1016/j.asr.2018.03.024

Ray K., Sen B. & Sharma P. (2016). Monitoring convective activity over India during pre monsoon season-2013 under the SAARC STORM Project. *Vayu Mandal* **42**(2): 106–128. DOI: http://imetsociety.org/wp-content/pdf/vayumandal/2016422/2016422_5.pdf

Rienecker M.M., Suarez M.J., Gelaro R., Todling R., Bacmeister J., Liu E. & Woollen J. (2011) MERRA: NASA's modern-era retrospective analysis for research and applications. *Journal of Climate* **24**(14): 3624–3648. DOI: https://doi.org/10.1175/JCLI-D-11-00015.1

Roy Bhowmik S.K., Sen Roy S. & Kundu P.K. (2008). Analysis of large scale conditions associated with convection over the Indian monsoon region. *International Journal of Climatology* **28**: 797–821. DOI: https://doi.org/10.1002/joc.1567

Schultz P. (1989). Relationships of several stability indices to convective weather events in Northeast Colorado. *Weather and Forecasting* **4**: 73–80. DOI: https://doi.org/10.1175/1520-0434(1989)004<0073:ROSSIT>2.0.CO;2

Sen Roy S. & Sen Roy S. (2021). Spatial patterns of long-term trends in thunderstorms in India. *Natural Hazards* **107**: 1527–1540. DOI: https://doi.org/10.1007/s11069-021-04644-6

Srinivasan V., Ramamurthy K. & Nene Y.R. (1973). Summer Nor'westers and Andhis and large scale convective activity over peninsula and central parts of the country. In: *Forecasting Manual Part - III: Discussion of Typical Synoptic Weather Situation.* India Meteorological Department, New Delhi, India.

The Hindu (2023). Lightning strikes claim 907 lives in 2022, highest toll in 14 years. Available at *https://www.thehindu.com/news/national/kerala/lightning-claims-907-lives-in-2022-highest toll-in-14-years/article66330661.ece*.

Tyagi B. & Satyanarayana A.N.V. (2019). Assessment of difference in the atmospheric surface layer turbulence characteristics during thunderstorm and clear weather days over a tropical station. *SN Applied Sciences* **1**(8): 909. DOI: https://doi.org/10.1007/s42452-019-0949-7

Tyagi B., Naresh Krishna V. & Satyanarayana A.N.V. (2011). Study of thermodynamic indices in forecasting pre-monsoon thunderstorms over Kolkata during STORM pilot phase 2006–2008. *Natural Hazards* **56**: 681–698. DOI: https://doi.org/10.1007/s11069-010-9582-x

Wilks D.S. (2006). *Statistical Methods in the Atmospheric Sciences*. 2nd edition. Academic Press, London, UK.